Adv Syst Sci Appl 2019; **02**; 120-133
Published online at http://ijassa.ipu.ru/index.php/ijassa/article/view/593

Optimal Rotor Design of Claw-Pole Alternator for Performance Improving

N.Brahimi[*1], S.Tahi[2], E. Boudissa[1], M.Bounekhla[1]

1) Laboratoire de Système Electrique et Télécommande, Université BLIDA 1, Blida, Algeria.

E-mail: nouzha_m74@yahoo.fr

2) Electrical and Industrial Systems Laboratory, USTHB/FEI, Algiers, Algeria.

E-mail: stahi@usthb.dz

Received May 17, 2018; Revised June 21, 2019; Published July 10, 2019

Abstract: The demand in electric energy, in vehicles, has experienced a remarkably rapid growth for a long time and this trend is expected to remain during the incoming years. The claw pole alternator is designed to provide the necessary power for all the electrical accessory loads over the entire operating speed, ranging from an idle speed of 1800rpm to a top speed of 6000 rpm. Because of the relationship between the speed and the output power, producing enough power at idle speed becomes a challenging problem. The aim of this paper is to optimize the rotor design of conventional claw pole alternator in order to improve its performance during the idle speed. To derive the optimal rotor structure, cyclic coordinate method linked with magnetic equivalent circuit (MEC) model is used, including magnetic saturation effect and leakage flux. An Increase of up to 70% in output power at idle speed is demonstrated and significant improvements in performance over the whole speed range were observed.

***Keywords**:* Claw pole alternator, reluctance network, MEC model, electric generator, shape optimization, cyclic coordinate method.

1. INTRODUCTION

Automotive alternators are responsible for the generation of electricity in almost all vehicles using an internal combustion engine. They must be capable of powering all the relevant systems the vehicle requires during operation. Until now, the claw pole alternator constitutes the unique device responsible for the generation of electricity within a vehicle [4]. The main advantages of the claw pole alternator are its low cost and construction simplicity. Therefore, it is well adapted for industrial and mass production. However it suffers from low efficiency caused by high leakage flux [19] and poor output power [22]. Performance and efficiency vary widely depending on the alternator speed and load conditions [12]. Commonly, during idle speed (1800 rpm), the claw pole alternator isn't able to sustain active electrical loads for a reasonable amount of time without undue drain on the battery. Therefore, obtaining sufficient output power at idle speed is required.

Recently there has been a considerable amount of work into developing higher power alternators with improved performance. Some of this work has focused on designing a new model of alternators such as the new claw pole alternator where the DC-excited winding is located in the stator [10]. Another example is the doubly excited brushless claw pole alternator, where the hybrid excitation is achieved by ferrite permanent magnets suitably mounted on both the rotor and the stator in one hand, and a field winding in the stator on the other hand [5, 18]. Most of these new designs of alternators need a lot more development before they become a

[*] Corresponding author: nouzha_m74@yahoo.fr

mature technology with possible integration in the vehicle power generating system. Improved performances are also obtained by, simply, adding surface or interior permanent magnet to the conventional claw pole alternator. Several studies have been carried out on hybrid excitation claw pole alternators [13, 24, 25]. In hybrid excitation, at least two magnetization sources are present in the rotor. In addition to the DC excited wound field, permanent magnets are placed into the rotor to compensate leakage flux and to boost rotor flux. Permanent magnet increases the power density and efficiency [21], however their higher price undermines their usage [16]. Furthermore, current regulations and industry marketing policies push the development process cycle energetically less expensive and environment friendly. This tight context implies finding new technical solutions to keep the same efficiency without permanent magnets. For these reasons a lot of efforts are being spent to improve performance and efficiency by optimizing the design of an existing traditional (conventional) claw-pole alternator [8, 23].

This paper describes the rotor design optimization of an existing conventional claw pole alternator while keeping same stator design and the same alternator footprint, in an attempt to increase the output power under different load conditions at the idle speed. The design improvement is achieved by using the magnetic equivalent circuit (MEC), which is widely considered in literature [2, 7, 9]. It has been shown in [15] that MEC model helps to predict performance of claw pole alternator with high accuracy and minimum CPU computation-time. Optimal rotor is designed by using cyclic coordinate method. The optimization results which provide the optimized rotor geometrical dimensions are discussed. The performance and the output power of the optimal claw pole alternator over the entire speed range from idle speed of 1800rpm to top speed of 6000 rpm are presented.

2. 3D NONLINEAR MAGNETIC EQUIVALENT CIRCUIT MODEL

Claw-pole alternator mathematical modeling is complicated because the paths of the magnetic flux are 3D. Therefore, the analytical method of magnetic equivalent circuit (MEC) based on reluctance networks theory is used [6, 7]. The claw pole MEC model employed in this work has been developed by Rakotovao [17] and used for optimization by Albert et al [2]. This MEC model is less time consuming compared with numerical model based on finite element theory [9]. Thus, the MEC model is particularly suitable for optimization purpose [15]. In the MEC method, each flux path section is characterized by magnetic reluctance. The good estimate of reluctances is essential because it guarantees the precision of the model and its coherence during optimization. Accuracy of the MEC model also depends on the topology of the network [14].

2.1 Expression of Reluctances

When material saturation is taken into account, the reluctance is non-linear function of the flux, as shown in equation (2.1) [9]:

$$R = \frac{L}{\Phi} H\left(\frac{\Phi}{S}\right) \tag{2.1}$$

where, L is the average flux path length, S is the cross-section area and Φ is the magnetic flux. H(B) is the analytical expression of the magnetic field versus the flux density B, which is expressed as follows [9]:

$$B = \frac{\Phi}{S} \tag{2.2}$$

2.2 Resolution Method of the MEC

Referring to the literature [9, 11], it has been reported that numerical resolution procedure of the claw pole MEC is based on Newton Raphson algorithm and reluctance network theory.

2.2.1 MEC resolution in No Load Condition

MEC resolution enables the evaluation of the fluxes circulating in the different parts of the magnetic circuit. In the case of no load condition, alternator's back electromotive force (back-EMF) is a function of the direct flux component only. The computation of the no-load back-EMF is expressed as follows [9]:

$$E = \frac{1}{\sqrt{2}} N_a \, \omega \, \Phi_m \tag{2.3}$$

where, N_a is the number of turns per armature phase, ω is the angular frequency and Φ_m is the maximum flux crossing a phase which is evaluated using the MEC resolution.

No-load back-EMF is plotted in Fig. 2.1, where it can be noticed that the magnetic saturation occurs when the field current is greater than 1A.

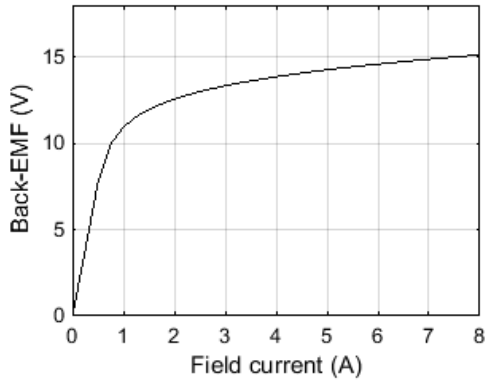

Fig. 2.1. No-load back-EMF EMF versus field current

2.2.2 MEC resolution under Load Condition

Claw pole alternator is a salient-pole synchronous generator with high saturated areas. Therefore, including the effect of the armature magnetic reaction in both q-and d-axis is required. Within the q-axis, magnetic saturation is low, resulting in a constant stator transverse inductance, while in the d-axis, saturation effect is important [2, 4]. Then, MEC accounting for the d-axis armature reaction is consider in order to carry out the flux linkage, especially, the one which allows the determination of the d-axis component of the back-EMF ( ), given by equation (2.3). Under load condition, the back-EMF phase is expressed in terms of its d and q components, as follows [9, 11]: $\underline{E}_d$

$$\underline{E} = \underline{E}_d + \underline{E}_q \tag{2.4}$$

with

$$\begin{cases} \|\underline{E}_d\| = E_d(I_f, I_d) \\ \|\underline{E}_q\| = X_q . I_q \end{cases} \tag{2.5}$$

where I_d and I_q are the d and q components of the armature current. I_f is the field current. X_q is the q-axis reactance.

Moreover, for resistive load and adopting Blondel model illustrated in Fig.2.2, the back-EMF: $\underline{E}$ is given by equation (2.6) [2, 4]:

$$\underline{E} = \underline{V} + R_s \underline{I} + jX_\sigma \underline{I} \tag{2.6}$$

where:

- R_s and X_σ are the phase resistance and leakage reactance respectively.
- R_L is the resistive load.
- $\underline{V}$ and $\underline{I}$ are voltage phasors and the armature current respectively.

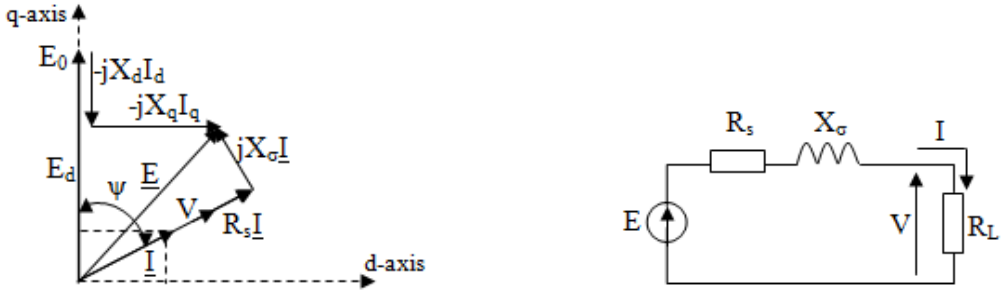

(a) (b)

Fig.2.2. (a) Blondel phase diagram in the case of resistive load. (b) Claw Pole alternator phase equivalent circuit.

Procedure for an operating point calculation is illustrated in Fig 2.3. At each step, the change in the solution is monitored. The process continues either until the change is less than the Newton Raphson tolerance of 0.1%. The solution is obtained, in several seconds, after maximum ten iterations.

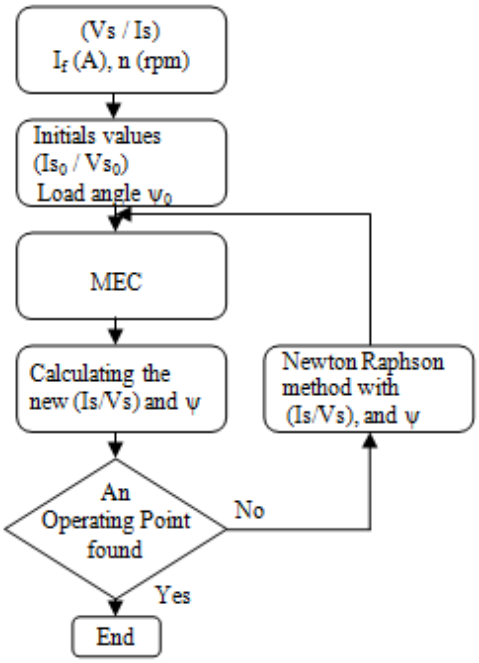

Fig.2.3. Operating point calculation algorithm.

3. ALTERNATOR PERFORMANCE

In the following section the alternator performances are evaluated across the whole speed range. The 1800 rpm speed corresponds to idle speed and 6000 rpm corresponds to cruising speed. Figure 3.1 (a) shows the calculated alternator output voltage versus the field current, parameterized by the load current. The alternator generated voltage increases along with

alternator speed and the field current. At idle speed, the maximum current drawn from the alternator is 20.62 A, with field current and output voltage are equal to 5A and 12VAC respectively. At this operating point, the saturation is well considered. It can be observed that when the load current increases the output voltage drops.

3.1 Armature Current Characteristic

The calculated armature current versus alternator speed is illustrated in Fig.3.1 (b). The field current is set to 5 A. The armature current curve is characterized by three operating point. The first one is the generation starting speed (P_{GS}) or 0-Ampere-speed at which the alternator reaches its rated voltage without delivering power. The second one is the maximum output current at cruising speed (P_C), which corresponds approximately to the short-circuit current of the alternator. The third one is the output current at idle speed (P_I)[12].

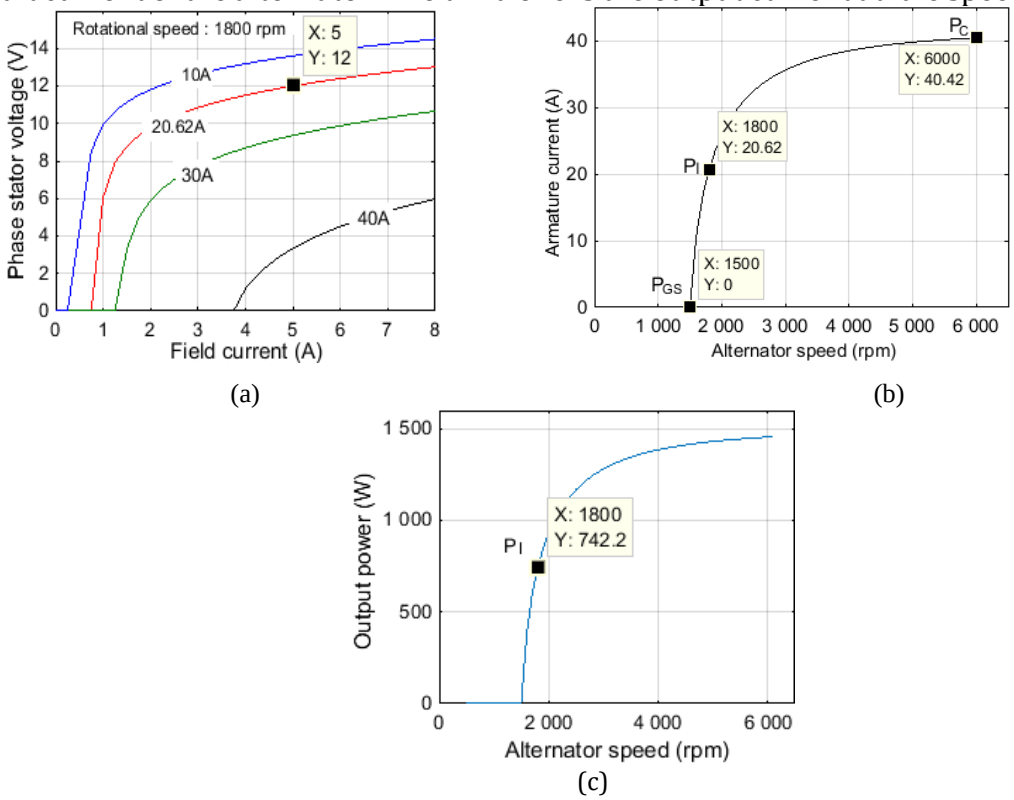

Fig. 3.1. (a) Stator phase voltage versus field current. (b) Armature current versus speed and the three operating points. (c) Output power versus speed at fixed output voltage

3.2 Alternator Output Power at Fixed Output Voltage:

Particular attention is paid to the output power requirement at idle speed, at which, the alternator must deliver at least the power needed for long-term consumers. No output power is required below the idle speed. The calculated output power curve versus alternator speed is shown in Fig.3.1. (c).

3.3 Maximum Output Power of the Alternator.

The calculated maximum output power of the alternator is given in Fig. 3.2. The field current is set to 5A. Figure.3.2 (a) shows the load current that corresponds to the maximum power delivered from the alternator. Figure.3.2 (b) shows the output voltage that corresponds to the maximum power. These curves show the amount of maximum available output power of the alternator.

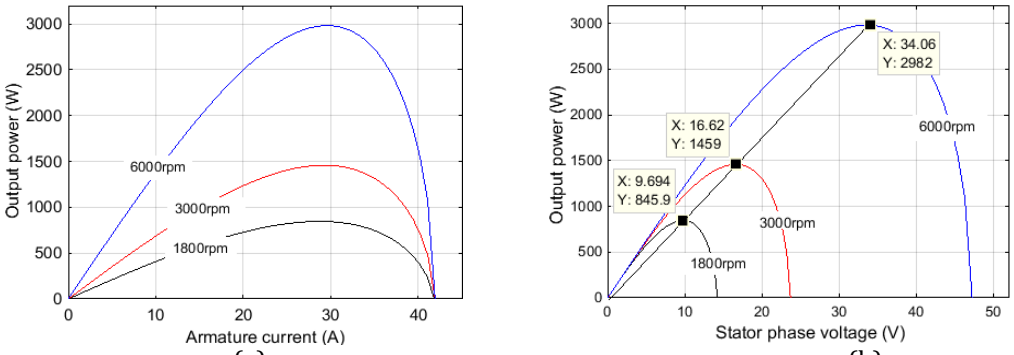

Fig.3.2. Calculated alternator output power parameterized by the alternator speed, versus (a) armature current, (b) stator phase voltage.

4. OPTIMIZATION DESIGN PROCEDURE

The aim is to optimize rotor structure of claw pole alternator at idle speed, including the magnetic saturation effect, while maintaining the same initial alternator footprint. The stator design parameters remain unchanged. Table 4.1 reports the alternator parameters, with assigned constant values that do not change during the optimization process.

Two optimization procedures are described, namely:

First optimization procedure

In the first optimization procedure, the objective function is to maximize the output power at idle speed while maintaining the output voltage at 12VAC. In this case, maximizing the output power leads to maximizing the delivered armature current.

Second optimization procedure

In the second optimization procedure, the objective function is to maximize the output power without imposing the output voltage or armature current.

Table 4.1. Main fixed parameters of the CPA.

Fixed parameter	Value
Number of phases	3
Number of pairs of poles	6
Number of stator slots	36
Outer stator diameter (mm)	127
Inner stator diameter (mm)	88.6
Shaft diameter (mm)	18.1
Height of plateau (mm)	11.95
Length of Rotor (mm):	52

4.1 Rotor Parameters Optimization

- *First optimization procedure*

Five crucial geometrical optimization parameters are selected, as shown in Table 4.2 and illustrated in Fig 4.1. Some of these geometrical parameters determine the shape of the claw pole. Determining the shape of the claw pole is the most important obstacle in the claw pole alternator designing process. The claw pole has an important role in closing the magnetic field lines because it ensures the route from the rotor excitation towards the air gap. The parameter, related to rotor core (core length) is, also, very important, especially as it conditions the space booked for the field winding.

- *Second optimization procedure*

In this case, besides the five geometrical optimization parameters, the armature current comes to be added as the sixth optimization parameter.

Table 4.2. Design of the sixth optimization parameters of the claw pole rotor

	Optimization variable	Optimization parameter	Base value (mm)
Geometrical optimization parameters	X_1	Width of the base of the claw	24.7
	X_2	Height of claw tip	4.7
	X_3	Core length	29
	X_4	Air gap length	0.65
	X_5	Width of claw tip	6
—	X_6	Armature current	—

In addition to these optimization parameters, there are other five geometrical implicit parameters, listed in Table 4.3 and illustrated in Fig 4.1. To ensure the geometrical coherence of the rotor, these parameters are subject to change according to optimization parameters evolution during the optimization process.

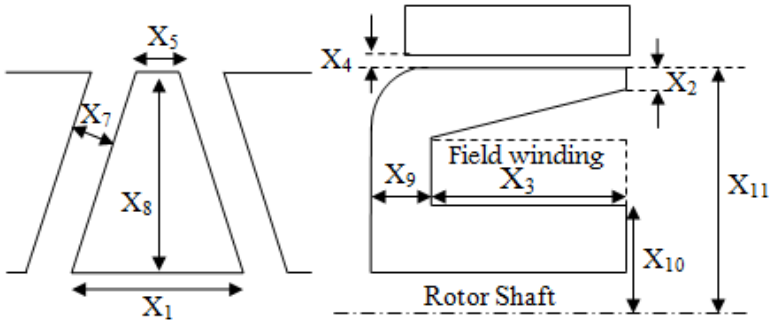

Fig.4.1. Geometrical parameters of rotor pole structure

Table 4.3. Implicit optimization parameters of the claw pole rotor

Implicit variable	Implicit parameter	Base value (mm)
X_7	Distance between claw	6.6
X_8	Claw pole length	29
X_9	Claw side plate thickness	11.5
X_{10}	Core radius	41.4
X_{11}	Outer rotor radius	87.3

The optimization of the rotor claw pole is a multivariable non-linear problem. In this investigation, the objective functions cannot be expressed as closed forms thus a derivative free optimization method is used for the objective function evaluation. Therefore, cyclic coordinate method is applied.

4.2 Cyclic Coordinate Method

A cyclic coordinate method [3, 20, 26] using the unknown parameters as the search directions, is applied to maximize the objective function successively along each coordinate. More specifically, the method searches along the directions d_1,....., d_n , where d_j is a vector of zeros except for a one at the j^{th} position. Thus, along the search direction d_j , the design variable x_j is changed while all other variables are kept fixed.

This technique is described in Fig. 4.2 for the first iteration and in the case of two coordinate axes X_1 and X_2. Starting from P_0 (X_{10}, X_{20}), the maximization is performed successively along X_1 and X_2 and leads, respectively, to P_1 (X_{11}, X_{20}) and P_2 (X_{11}, X_{21}). The iterative process is repeated until the error test is satisfied. The algorithm shown in Fig. 4.3,

estimates the vector parameters P that maximizes the objective function which increases at each iteration.

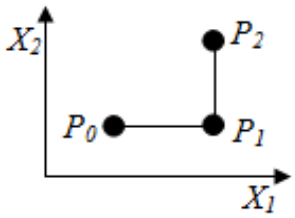

Fig.4.2. 2-D illustration of the cyclic algorithm

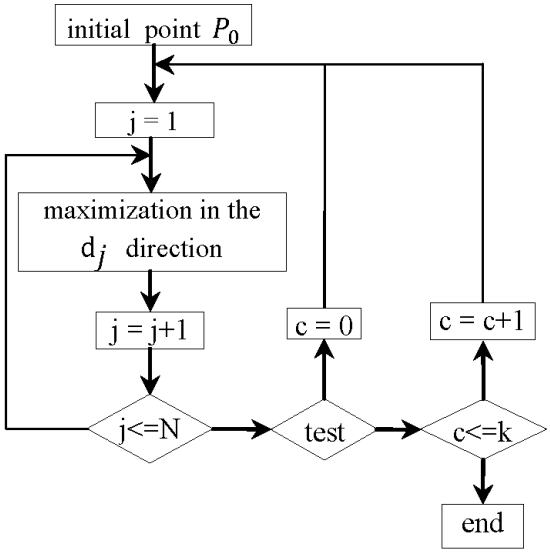

Fig.4.3. Flowchart of the cyclic coordinate algorithm

In this study, the alternator output power is chosen as objective function, which is expressed as follows [22]:

$$P = 3 * V_0 * I_s \tag{4.1}$$

where, P is the output power, V_0 and I_s are the RMS value of output voltage alternator and armature current respectively. Both speed and field current are kept constant and equal to-1800 rpm and 5A respectively. Orientation of the optimal solution toward a technically correct solution requires us to limit the search space. Therefore, the optimization variables are constrained to vary in a range, between a lower and an upper limit, as shown in Table4.4. The armature current is introduced, only in the second optimization procedure, as a sixth variable.

Table 4.4. Optimization variables (mm or A).

Optimization variable	Lower limit	Upper limit
X_1	0.3	0.65
X_2	1	5.5
X_3	25	29
X_4	6	38.02
X_5	3	10
X_6	10	80

5. OPTIMIZATION RESULTS AND COMMENTARIES

As expected, using MEC coupled with cyclic coordinate method yields results, a few iterations (about 1h30) are required to achieve the maximum of the objective function. Cyclic coordinate is a deterministic method, thus it is appropriate to secure the obtained results. This is done by using different sets of initial points and to check if the same maximum output power is obtained. Figure.5.1 (a) and Fig.5.1 (b) show the evolution of the objective function. The results of the optimal geometrical dimension of the rotor parameters are summarized in Table 5.1 and Table 5.2.

- *First optimization procedure :*

The output power, at idle speed, increases from 0.742 kW to around 1.27 kW which constitutes 71.15% improvement. The armature current increases from 20.62 A to 35.27 A.

- *Second optimization procedure:*

At idle speed, the maximum output power reaches 1.3KW which constitutes 53.68% improvement.

Table 5.1. First optimization procedure, base and optimized values of design variables

Optimization parameter	Value before optimization (mm)	Value after optimization (mm)
Air gap length	0.65	0.3
Height of claw tip	4.7	1
Core length	29	25
Width of the base of the claw	24.7	23.13
Width of claw tip	6	4.35
Implicit parameter		
Distance between claw	6.6	8.7
Claw pole length	29	25
Claw side plate thickness	11.5	13.5
Core radius	41.4	42.1
Outer rotor radius	87.3	88

Table 5.2. Second optimization procedure, base and optimized values of design variables

Optimization parameter	Value before optimization (mm or A)	Value after optimization (mm or A)	Difference in parameter value (between 1st and 2nd optimization) (mm)
Air gap length	0.65	0.3	0
Height of claw tip	4.7	1	0
Core length	29	25	0
Width of the base of the claw	24.7	23.94	-0.81
Width of claw tip	6	4.17	0.18
Armature current	29.08	32.09	—
Implicit parameter			
Distance between claw	6.6	8.4	0.3
Claw pole length	29	25	0
Claw side plate thickness	11.5	13.5	0
Core radius	41.4	42.2	0.1
Outer rotor radius	87.3	88	0

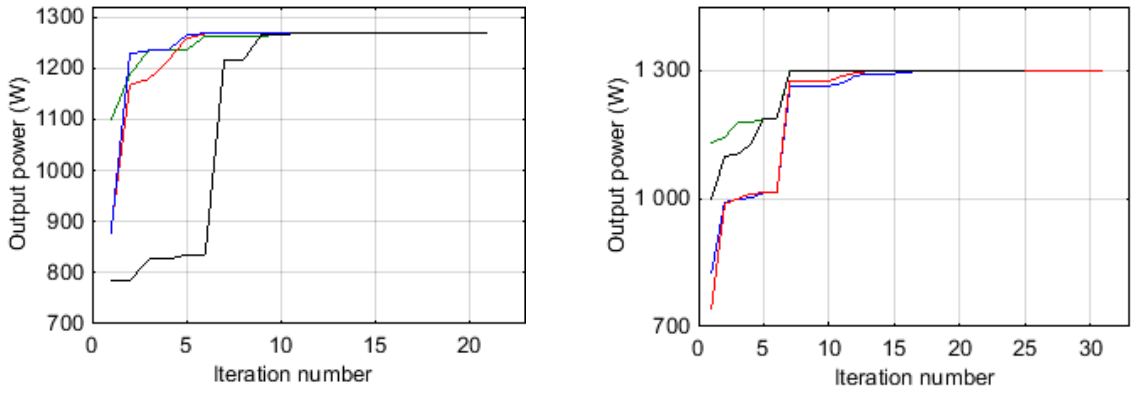

(a) (b)

Fig.5.1. Evolution of output power versus number of iteration for the (a) first optimization procedure. (b) second optimization procedure.

- *Impact of the air gap length:*

The air gap length can affect the output power considerably. In theory, to maximize the output power of an alternator, the air gap length should be designed as small as possible. For a typical alternator, the nominal air gap is approximately 0.4 mm but it can be larger or smaller. When the air gap is reduced, the output power is substantially improved [1]. However, the air gap of a claw-pole alternator should not be designed too small. When running at very high speeds, the alternator rotor poles will deflect due to centrifugal forces and the pole tip will touch the stator. In this investigation, the optimization process, can give solutions for very small values of the air gap, but the technically feasible solution selected is the one which corresponds to the air gap lower limit given above. The air gap flux is increased from 2.627 10^{-4} Wb to 3.333 10^{-4} Wb.

- *Impact of the width of the base of the claw and the width of claw tip:*

These two parameters, determine the exchange surface between rotor and stator through the air gap. It is important to recall that, the magnetic radial flux is more concentrated at the basis of the claw pole than at its extremity. Hence, the radial fluxes increases when the width of the base of the claw pole increases. However, the leakage fluxes between two adjacent claw poles, which are the most important leakage fluxes, increase when the width of the base of claw increases. The optimization process gives the optimal value of these two variables which lead to the maximum output power. In Table 5.3, one can observe the reduction of the leakage flux between two adjacent claw poles and leakage flux between claw pole tip and opposite plate.

- *Impact of the height of claw tip:*

The leakage fluxes between the claw pole and rotor winding can be affected by this parameter. To reduce these leakage fluxes, the distance between rotor core and the bottom of the claw should be designed as far as possible. This explains the fact that the optimal value of this variable tends to the lower limit given above. Table 5.3 shows the reduction of the leakage flux between the claw pole and rotor winding.

- *Impact of the core length:*

The optimization process assigns the lower limit to this variable. However, what is lost in length will be gained in claw side plate thickness. As a result, the junction who binds the core to the claw side plate is larger which enables more axial flux to be captured.

Table 5.3. Leakages fluxes before and after optimization

Leakage fluxes	Base value (*10^{-4} Wb)	Value after optimization (*10^{-4} Wb)
between adjacent claw pole fingers	1.1286	0.6855

between claw pole and rotor winding	0.04016	0.02449
between claw pole tip and opposite plate	0.02933	$4.5953\ 10^{-6}$

6. ALTERNATOR PERFORMANCE AFTER OPTIMIZATION

After optimization process, the output performances of the optimal claw pole alternator are evaluated. In Fig. 6.1(a) and Fig. 6.1 (b) the armature current and output power, are respectively plotted versus the rotational speed. It can be seen that, at idle speed of 1800rpm, optimized rotor design leads a higher armature current and hence to a higher output power. Figure 6.1 (c) illustrates that only 1A field current is needed to deliver current at idle. In Fig.6.2, (a) and (b) the maximum output power reaches 1.3 kW at idle speed. It can be observed that output performances of the optimazed alternator has been improved in the whole speed range from idle speed of 1800rpm to the cruising speed of 6000rpm. At the cruising speed of 6000 rpm the maximum output power reaches 4.5 kW.

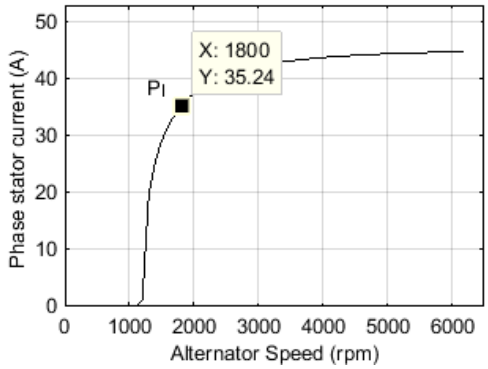

(a)

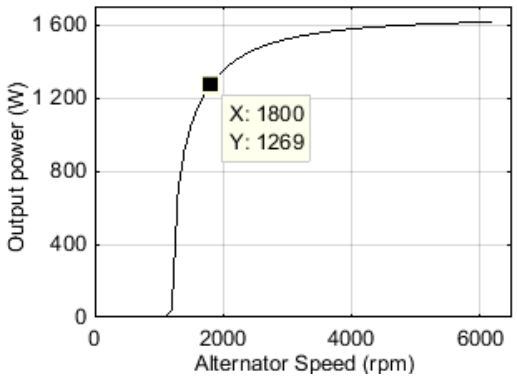

(b)

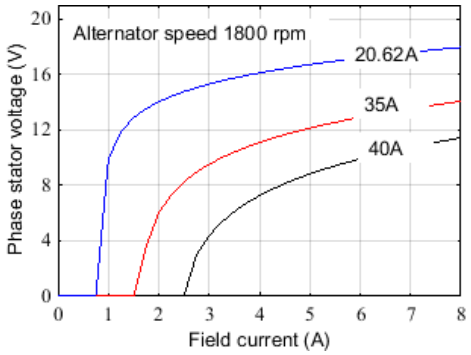

(c)

Fig. 6.1. (a) Stator phase current versus alternator speed. (b) Alternator output power versus alternator speed. (c) Stator phase voltage versus field current.

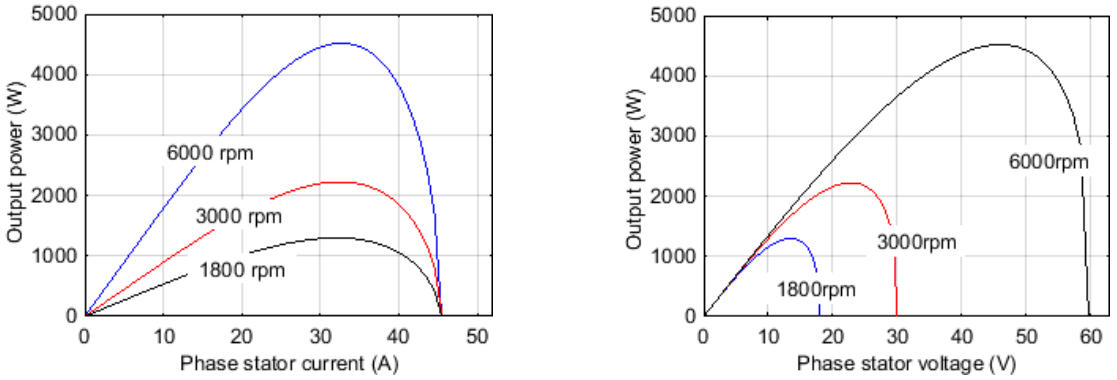

(a) (b)

Fig. 6.2. (a) Output power versus Armature current. (b) Output power versus stator phase voltage.

7. CONCLUSION

In this paper, the optimization method based on cyclic coordinate method coupled with magnetic equivalent circuit (MEC) model, has been applied successfully for the design of rotor claw pole alternator. The main objective was to maximize the alternator output power for given stator dimensions and footprint at the idle speed of 1800rpm.

The output power increased significantly at idle speed, it was demonstrated that output power and armature current of the optimized claw-pole alternator increased from 0.742 kW to 1.27 kW and from 20.62 A to 35.27A, which constitute 71.15% and 71.04% improvement, respectively. This is predominantly due to change in reluctance of geometric parameters, consequently affecting the flux throughout the alternator.

At idle, the maximum output power delivered from the optimized alternator achieved 1.3 kW which constitutes 53.68% improvement.

The obtained results indicate significant performance improvement of the optimized alternator over the whole speed range (1800 rpm to 6000 rpm), whereas the geometry optimization process has been fully concentrated at the idle speed. At high speed of 6000 rpm, the maximum available output power increased from 2.9 kW to 4.5 kW, a 50.90% improvement

Future investigation would consider the use of the MEC model in the design optimization of various generators taking advantage of the claw-pole structure in harvesting energy systems.

REFERENCES

[1] Alaeddini,A., Darab, A., & Tahanian, H., (2015). Influence of Various Structural Factors of Claw-Pole Transverse Flux Permanent Magnet Machines on Internal Voltage using Finite Element Analysis. *Serbian Journal of Electrical Engineering*, 2 (12), 129-143. DOI: 10.2298/SJEE1502129A

[2] Albert, L., Chillet, C., Jarosz, A. & Wurtz, F., (2003). Analytic modeling of automotive claw-pole alternator for design and constrained optimization. *10th Eur. Conf. Power Electronics and Applications, in Processing*, Toulouse, France.

[3] Bazaraa M.S., Sherall H.D. & Shetty C.M., . (1993). *Nonlinear programming Theory and Algorithms*, John Wiley & Sons, Inc.

[4] Boldea, I., (2006). *Variable Speed Generators*. CRC Press, Taylor & Francis Group, second edition, Boca Raton.

[5] Dajaku, G., Lehner, B., Dajaku, Xh., Pretzer, A. & Gerling, D. (2016). Hybrid Excited Claw Pole Rotor for High Power Density Automotive Alternators. *Electrical Machines (ICEM), XXII International Conference of the IEEE*, Lausanne, Switzerland.

[6] Delale, A., Albert, L., Gerbaud, L. & Wurtz, F. (2004). Automatic Generation of Sizing Models for the Optimization of Electromagnetic Devices Using Reluctance Networks. *IEEE Transactions On Magnetics*, 2 (40), 830-833.

[7] Hecquet,M. & Brochet,P., (1995) Modeling of a Claw-Pole Alternator Using Permanence Network Coupled with Electric Circuits, *IEEE Transactions on Magnetics*, Vol 31, N°3,2131-2134.

[8] Hidaka,Y. & Igarashi, H. (2018). Three dimensional shape optimization of claw pole Motors. *J. Adv. Simulat. Sci. Eng*., 1 (4), 64-77.

[9] Ibala, A., Rabhi, R., & Masmoudi, A. (2011). MEC-Based Modeling of Claw Pole Machines: Application to Automotive and Wind Generating Systems. *International Journal Of Renewable Energy Research, IJRER*, 3 (1), 1-8.

[10] Ibala, A. & Masmoudi, A. (2010). Accounting for the Armature Magnetic Reaction and Saturation Effects in the Reluctance Model of a New Concept of Claw-Pole Alternator. *IEEE Transactions on Magnetics*. 11 (46), 3955 – 3961. DOI**:** 10.1109/TMAG.2010.2055882

[11] Ibala, A. & Masmoudi, A. (2015). MEC-based prediction to the loss of claw pole alternators, *The Inter. Journal for Computation and Mathematics in Electrical and Electronic COMPEL*, 6 (34), 1719 – 1730. http://dx.doi.org/10.1108/COMPEL-06-2015-0216.

[12] Ivankovic, R., Cros, J., et al., (2012). Power Electronic Solutions to Improve the Performance of Lundell Automotive Alternators. *New advances in vehicular technology and automotive engineering*. InTechOP ISBN: 9535106982.

[13] Jurca, F.N. & Martis, C. (2012). Theoretical and experimental analysis of a three-phase permanent magnet claw pole synchronous generator. *IET Electric Power Applications*, 8 (6), 491-503.

[14] Moallem, M. & Dawson, G.E., (1998), An Improved Magnetic Equivalent Circuit Method for Predicting the Characteristic of Highly Saturated Electromagnetic Devices. *IEEE Transactions on Magnetics*, 5 (34) , 3632-3635.

[15] Ostovic, V., Miller, J.M., K.Garg, V., Schultz, R.D. and Shawn, H. (1999). A magnetic equivalent circuit based performance computation of a Lundell Alternator, *IEEE transaction on industry application*, 4 (35)

[16] Perez, S., (2013), Contribution au dimensionnement optimal d'alternateur à griffe sans aimants Apport des alliages FeCo [Contribution to Optimal Sizing of Claw-Pole Alternator Without Magnet- Contribution of FeCo Alloys], *PhD thesis*, EDEEATS, Grenoble, France. [in French].

[17] Rakotovao, M.,(1993), Un modèle operationnel complet pour l'alternateur à griffe [A Complete Operational Model For Automotive Claw-Pole Alternator], *PhD thesis*, Cachan France, [in French]

[18] Rebhi, R., Ibala, A. & Masmoudi, A. (2013). On the Modeling of a Doubly-Excited Brushless Claw Pole Alternator: Application to a Solar-Wind-Wave Hybrid Energy Conversion System, *Eighth International Conference and Exhibition on Ecological Vehicles and Renewable Energies,* EVER, Monaco, DOI**:** 10.1109/EVER.2013.6521547

[19] Sharma,A., (2013),Use of Anisotropic Materials In Claw-Pole Alternator to reduce Leahage Flux, *Proc. Annual IEEE India Conference (INDICON*),India DOI**:** 10.1109/INDCON.2013.6725997

[20] Tahi, S., Ibtiouen, R. & Bounekhla, M. (2011). Design Optimization of Two Synchronous Reluctance Machines Structures With Maximized Torque and Power Factor, *Progress In Electromagnetic Research B*, 35, 369–387.

[21] Upadhayay,P., Lebouc, A.K., Garbuio, L., Mipo, J.C. & Dubus, J.M., (2017), Design & Comparison of Conventional & Permanent magnet based Claw-Pole Machine for Automotive Application, *Proc. of the 15^{h} Int. Conf. on Electrical Machine (ELMA)*, sofia, Bulgaria, DOI**:** 10.1109/ELMA.2017.7955390

[22] Whaley, D.M., Soong, W.L. & Ertugrul, N. (2004). Extracting more power from the Lundell car alternator, Australasian Universities *Power* Engineering Conference, AUPEC, Brisbane, Australia.

[23] Xiao-hual, Bao & Liu Mou-zhi, (2012). Parameter analysis and optimal design for mobile Claw-pole alternator, *Applied Mechanics and Materials* Vols. 130-134, 658-661, *Trans Tech Publications*, Switzerland.

[24] Xiaohua Bao, Qingling He, Qunjing Wang & Youyuan Ni, (2008). Research and Optimal Design on Hybrid Excitation Claw-pole Alternator for Automobile Application, *Electrical Machines and Systems, IEEE International Conference*, 3493- 3496, ICEMS, Wuhan, China.

[25] Zhenyang Zhang, Huijuan Liu & Tengfei Song, (2016), Optimization Design and Performance Analysis of a PM Brushless Rotor Claw Pole Motor with FEM, *Machines, MDPI*, 3 (4).

[26] Zaïm M. E., Dakhouche K. & Bounekhla M., (2002). Design for torque ripple reduction of a three-phase switched reluctance machine, *IEEE Transactions on Magnetics*, 38(2): 1189–1192.